

**Chapter 7 –**

**Effects of aspartame on the morphology and  
count of the different leukocytes and the ultra-  
structure of the endothelial lining of the aorta of  
the rabbit**

## **RESEARCH QUESTION 5:**

Has the morphology and number of the leukocytes (light microscopy) changed after treatment with aspartame and how is the endothelial lining (SEM and TEM) of the blood vessels affected when treated with aspartame?

### **7.1 INTRODUCTION**

The blood coagulation system does not only consist of coagulation factors, fibrin networks and platelet aggregates which is in constant equilibrium, but also cells and plasma. Blood itself consists out of plasma, erythrocytes and leukocytes. The plasma contains all the circulating coagulation factors and proteins needed to form fibrin networks and for release of platelet granules to form platelet aggregates. The erythrocytes are necessary for transport of oxygen, while the leukocytes play a key role in the immune system. The blood vessels through which the blood flows also forms an integral part of this whole system in equilibrium as it forms part of the intravascular anti-coagulation mechanism. Thus, having focussed on the effects of aspartame on the coagulation factors (Chapter 5), fibrin networks and platelet aggregates (Chapter 6), the aim of this chapter was to determine the effects of aspartame on the leukocytes (morphology and count) and the endothelial lining.

Most of the leukocytes in rabbits and guinea pigs appear very similar to those of other mammals. Novices may easily mistake heterophils (lapine and cavian equivalent of neutrophils) for eosinophils. Heterophils have the same function as other mammalian neutrophils, but they have acidic or eosinophilic granules in their cytoplasm. They are sometimes referred to as “pseudoeosinophils” in the literature. Heterophils are present in a number of animal species including birds, reptiles, amphibians, some fish, rabbits, guinea pigs and hamsters. The functions of the leukocytes of rabbits are similar to those of other mammals, including humans (Lester, Tarpley and Latimer, 2005).

Zhang and co-workers in 1995 used scanning and transmission electron microscopy to determine the influence of 5-fluorouracil on the endothelium in small arteries of rabbits. 5-Fluorouracil (5-FU) is a widely used antieoplastic agent. 5-FU induced cardiotoxicity is still a relatively unknown side-effect of this drug. This phenomenon could be due to a direct cytotoxic effect on the endothelial cells. Zhang and co-workers tested this hypothesis in an experimental

study in rabbits, by scanning or transmission electron microscopic evaluation of endothelium in small arteries (the central artery of the ear) after *in vivo* treatment with 5-FU. Both local and systemic effects of 5-FU on endothelium were studied 15, 30, 60 and 120 minutes after intra-arterial or intraperitoneal treatment. Perfusion fixation at physiological pressure and temperature was used in order to minimize damage to the endothelium during the preparation procedure. Irreversible cell damage was observed with 5-FU treated animals with disruption of the endothelial sheet and patchy exposure of the subendothelium, sometimes as focus for thrombus formation.

A quantitative SEM analysis was performed to determine the degree of injury to the endothelium of the rabbit aorta and carotid artery during experimental arteriosclerosis (Zaikina *et al.*, 1982). The luminal surface of the aorta and the carotid artery in normal and cholesterol-fed rabbits was studied by scanning electron microscopy. To study the endothelial injury the vessels were perfused and stained under physiological pressure. The frequency of large and small endothelial defects was determined per surface unit of endothelium in the normal and experimental groups of rabbits. Loss of endothelial cells was regarded as a large defect, argyrophilic cells, craters, and stomata were regarded as small ones. It was found that the percentage of regions without endothelial cells was similar in both control rabbits and in rabbits with experimental atherosclerosis. The frequency of small endothelial defects increased in rabbits after 3 weeks of hypercholesterolemia but decreased to the control level after 6 weeks of hypercholesterolemia. In rabbits with 8 months of hypercholesterolemia the frequency in defects outside the plaques did not differ from the control group. In the group with hypercholesterolemia for 8 months 39.2% of the plaque surface contained endothelial cells in which there were no distinct silver-stained cell borders. The data that was obtained do not support the assumption that morphological endothelial injury is the structural precursor of plaque formation.

## **7.2 MATERIALS AND METHODS:**

### **7.2.1 Light microscopy study of the leukocytes**

#### **7.2.1.1 Obtaining blood smears**

The rabbits utilized for the When the last concentration of aspartame was completed, blood smears were used to determine the accumulative effect of the aspartame on the leukocyte count and morphology. After 1.5ml blood was drawn from the different rabbits and before the samples were centrifuged for obtaining plasma for the Start 4 coagulation and SEM studies, droplets of blood was taken from each rabbit to obtain the blood smears. A droplet of blood was touched to the clean surface of the slide on the right hand side. Another slide was placed at a 20° angle on the first slide and to the left of the droplet of blood. The second slide was pulled to the right, till the droplet of blood touched this slide. When the blood was spread across the whole line of contact, the slide was pulled rapidly towards the left. This was done till all the blood disappeared or the other side of the slide was reached. The blood smears were air dried and stored till staining.

#### **7.2.1.2 Staining of blood smears:**

A combined Wright-Giemsa stain, developed by Wilcox in 1943, was utilized for staining of the blood smears (Humason, 1967). Giemsa powder was dissolved in glycerol and placed in an oven set at between 55-60°C for 2 hours, while stirring occasionally. The mouth of the flask was covered with a double layer of aluminium foil to prevent absorption of moisture. After the 2 hours were complete, aged Wright's staining solution (2 g per 1000ml Methanol) was added to the Giemsa solution. This solution was left to stand overnight and additional Wright's solution was added the following day. The Wright-Giemsa stock solution was then filtered. A buffer solution was obtained from two different solutions in distilled water. Solution A was dibasic sodium phosphate dissolved in distilled water and solution B monobasic potassium phosphate dissolved in distilled water. The buffer was then prepared by diluting 61.1ml of solution A and 38.9ml of solution B in 900ml distilled water. A working stain was then prepared from this Wright-Giemsa stock solution by using 1 part Wright-Giemsa stock solution in 9 parts buffer solution.

This staining method was further combined with another staining method for old smears (Humason, 1967). Before the blood smears were stained with the working Wright-Giemsa stain, the smears were treated for 7 minutes in an alcohol-acetic acid solution (10 drops glacial acetic acid to 60ml absolute alcohol). This causes the old smears to stain more brilliantly.

The slides were then stained with the working Wright-Giemsa stain for 10 minutes. The stain was flushed from the slide with the prepared buffer which prevents precipitate on slides. The slides were then submerged in buffer solution for 1 minute. The slides were air dried by standing them on end and mounted.

### ***7.2.1.3 Counting of blood smears***

All blood smears were placed on white tissue paper to accentuate the appearance of the smears. The smears that had the same appearance and had the same degree of staining were then used for leukocyte counting on a Nikon Optiphod transmitted light microscope (Nikon Instech Co., Kanagawa, Japan). Smears were counted till a hundred leukocytes were distinguished. The number of zones that were counted to obtain the hundred cells was noted. These two methods were combined due to the difference in the appearance of the individual blood smears.

## **7.2.2 SEM and TEM studies of the endothelial cells of the aorta**

### ***7.2.2.1 Termination of the study to obtain tissue***

After the treatment periods were completed, all the rabbits were euthanized by means of intraperitoneal injection with sodium pentobarbitonehydrochloride (2ml) by a skilled person experienced in this technique (Mrs Annette de Freitas, animal technologist at the Medunsa campus of the University of Limpopo). Five rabbits, 3 controls and 2 treated with aspartame (with negative/adverse clotting profiles) were dissected for the soft tissue of their livers and kidneys and the arch of the aorta (for SEM and TEM). The organs were fixed in formaldehyde and reserved for light microscopy studies (discussed in following chapter) and the arch of the aorta fixed in 2.5% glutaraldehyde and reserved for SEM and TEM studies.

### **7.2.2.2 Preparation of the aorta for SEM and TEM**

The dissected tissue was kept in the 2.5% glutaraldehyde and was kept at 8°C till preparation for SEM and TEM. Care was taken that the fixative was in contact with the tissue at all times. The tissue was removed from the fixative and washed three times with Na/K phosphate buffer for 15 minute washes. This was followed by post-fixing with osmium tetroxide (OsO<sub>4</sub>) (50% PO<sub>4</sub> buffer at pH=7.4 and 50% OsO<sub>4</sub> from a 1% stock solution) for an hour. The osmium tetroxide was removed from the tissue and three wash steps of 15 minutes each in Na/K phosphate buffer followed. The tissue was then dehydrated with different concentrations of ethanol and left in the last absolute ethanol wash. Tissue that was to be viewed with the SEM was then placed in the critical point dryer (Bio-Rad E3000; Watford, England).

Double-sided carbon tape was attached to bronze slides and the tissue was then placed onto the carbon tape. The slides were placed in a sputter coater (Polaron E5200C; Watford, England) and coated with Ruthenium (RuO<sub>4</sub> vapour from a 0.5% solution for 30 minutes) and were then ready for viewing under the JSM-840 (JEOL, Tokyo, Japan).

The sections of aorta that were to be viewed with the TEM (Phillips EM301; Eindhoven, Netherlands) was placed in Quetol resin (Quetol 651, cured at 60°C for 48 hours) and sectioned with an ultra-microtome (Reichert Ultracut E; Vienna, Austria). The sections were then coated with uranylacetate (to obtain contrast) for 30 minutes followed by a number of washing steps in 3 different washes of distilled water. The sections were then counter-stained with lead citrate for 3 minutes, followed with 3 washes of distilled water. The sections were then ready for viewing with the TEM (Phillips EM301; Eindhoven, Netherlands).

## **7.3 RESULTS AND DISCUSSION**

### **7.3.1 Light microscopic study of the morphology of the leukocytes**

Figure 7.1a and 7.1b compares the lymphocytes of the control and aspartame treated rabbits respectively.

**Figure 7.2:** Lymphocytes of a control rabbit (marked with circles) (Label a) compared to the lymphocyte of a rabbit treated with aspartame (Label b)

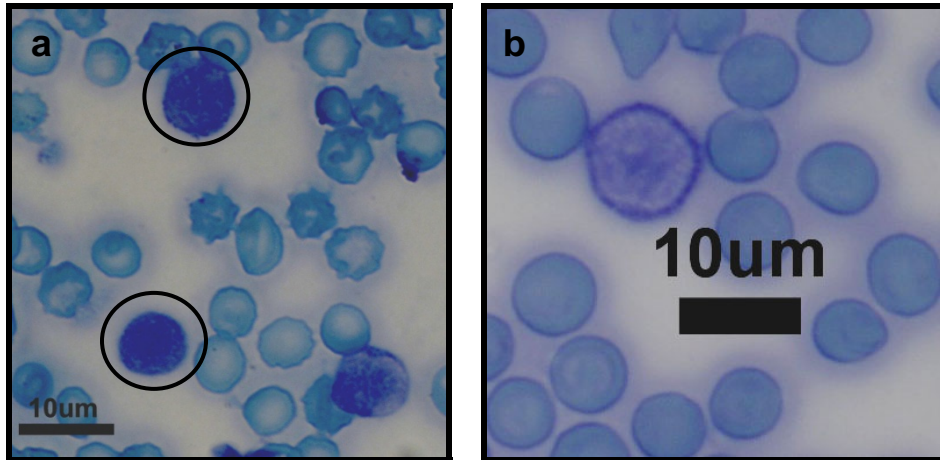


Figure 7.2a and 7.2b compares the monocytes of the control and aspartame treated rabbits.

**Figure 7.2:** Comparison between the monocytes of the control rabbit (marked with a solid circle; Label a) and the aspartame treated rabbits (Label b)

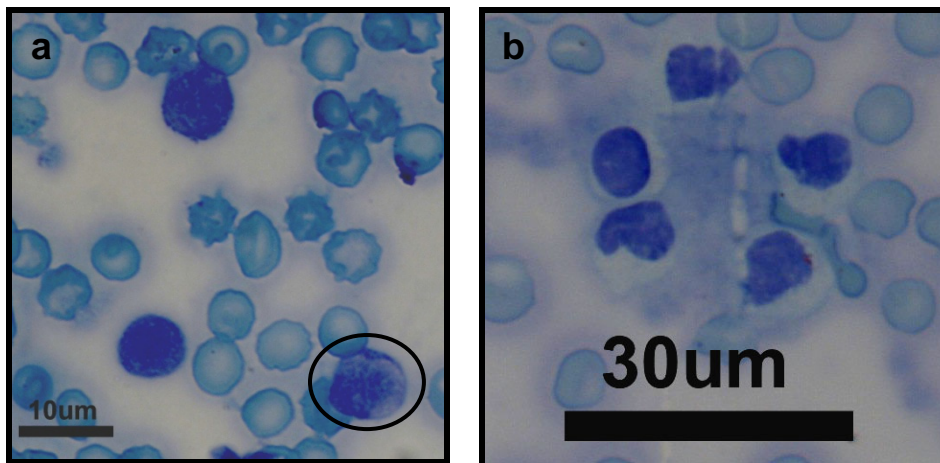


Figure 7.3a and 7.3b compares the basophils of the control and aspartame treated rabbits.

**Figure 7.3:** Comparison between the basophils of the control rabbit (Label a) and the aspartame treated rabbits (Label b)

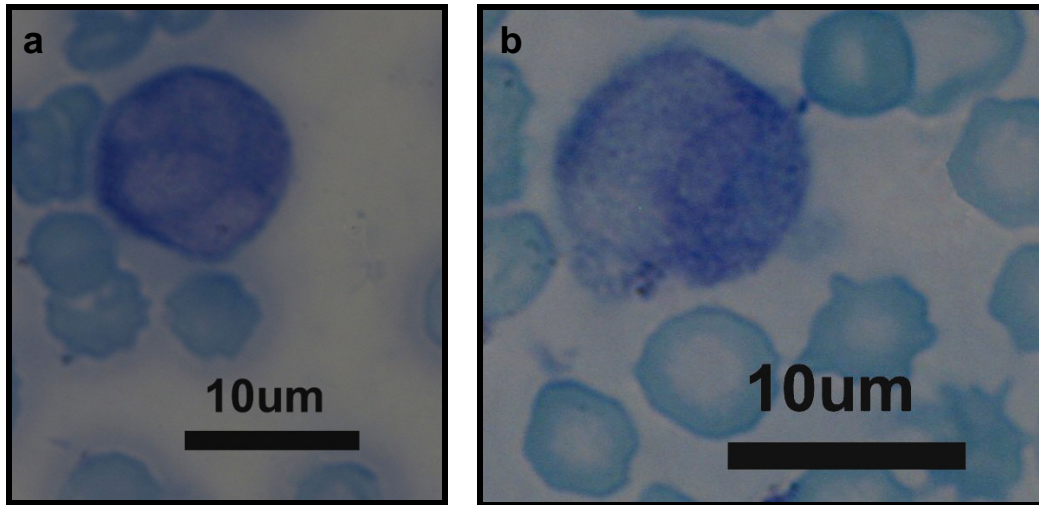


Figure 7.4a and 7.4b compares the eosinophils of the control rabbit and the aspartame treated rabbits respectively.

**Figure 7.4:** Comparison between the eosinophils of the control rabbit (inside the circle; Label a) and the rabbits after treatment with aspartame (Label b)

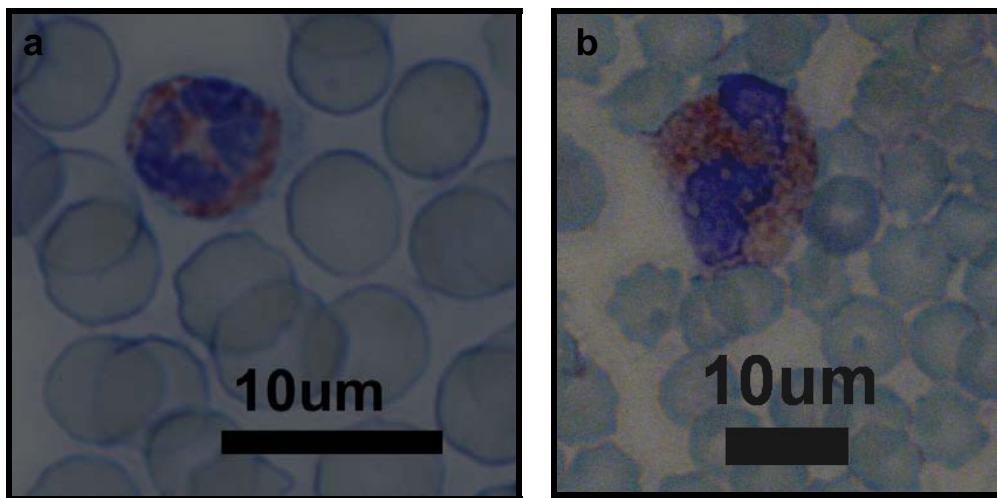
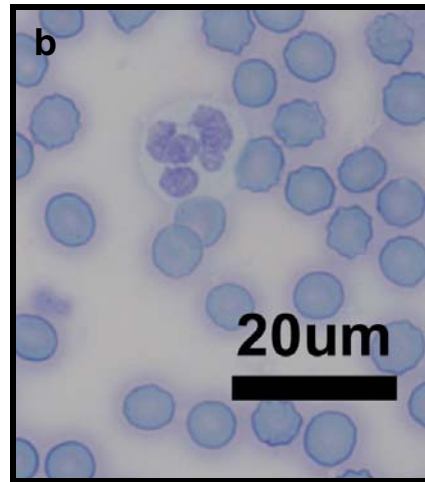
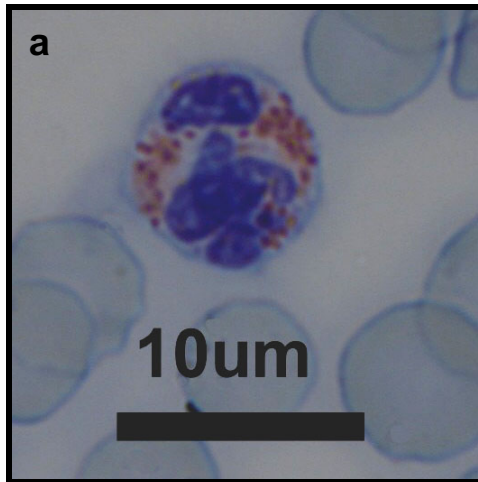


Figure 7.5a and 7.5b compares the heterophils of the control rabbit with that of the aspartame treated rabbits respectively.



**Figure 7.5:** Comparison between the heterophils of the control rabbit (Label a) and those of the rabbits after treatment with aspartame (Label b)



### **Morphology of the lymphocytes**

The nuclei of the lymphocytes of the control rabbits stained dark blue with very little cytoplasm visible (Figure 7.1a). The lymphocytes for the rabbits treated with aspartame (Figure 7.1b) stained lighter blue, with the cytoplasm closely related to the cell membrane staining darker blue, almost forming a halo around the nucleus. It appeared as though the control rabbits had more densely packed chromatin throughout the nucleus. No difference was noted in the size of the lymphocytes between the control and aspartame treatment groups.

### **Morphology of the monocytes**

The monocytes of the control rabbits possessed a dark staining nucleus with lighter areas of cytoplasm surrounding it. Densely packed chromatin was visible in the cytoplasm. A number of vacuoles could be seen as round white vesicles in the cytoplasm (Figure 7.2a). The size of the monocytes was not affected by the treatment with aspartame, but the morphology changed to a degree. The dark-blue stained nuclei could be distinguished quite easily with the characteristic bean-shape of the nucleus being prominent. The cytoplasm visible around the nucleus was larger and was almost transparent, not light blue like in the controls. No vacuoles were visible (Figure 7.2b). The cell membranes were clearly visible in both the control and aspartame treated rabbits.

### **Morphology of the basophils**

No difference could be seen between the basophils of the controls and aspartame treated rabbits. Both exhibited bi-lobar nuclei with distinct blue staining granules in the cytoplasm. The cytoplasm of the control did stain a bit darker than the cytoplasm of the aspartame treated cells. The cell membrane of the control was also more clearly distinguishable than that of the basophils obtained from rabbits that were treated with aspartame. The size of the basophils was not adversely affected by the aspartame treatment.

### **Morphology of the eosinophils**

The eosinophils of both the control and aspartame treated rabbit had the characteristic bi-lobar nuclei, with a distinct blue stain (Figure 7.4a and 7.4b). It appears as though the chromatin of the nucleus of the aspartame treated rabbits are more densely packed close to the nuclear envelope. The eosinophilic granules of the aspartame treated rabbits stained more brilliantly than that of the control (Figure 7.4b). There was no difference in the size of the cells after

treatment with aspartame. The cell membrane of the control rabbit was more clearly visible than that of the rabbits in the treatment group, staining light blue in colour.

### **Morphology of the heterophils**

The nuclei of the heterophils of both the control and aspartame treated rabbits stained brilliantly blue and up to five lobes could be distinguished (Figure 7.5a and 7.5b). The chromatin of the nuclei of the aspartame treated rabbits appeared more densely packed (Figure 7.5b). The red granules in the cytoplasm stained more brilliantly in the control rabbit (Figure 7.5a) than that of the aspartame treated rabbits and individual granules could be distinguished. The granules of the heterophils of the aspartame treated rabbits (Figure 7.5b) seem to be less and individual granules could not be as clearly distinguished as in the control. The size of the cells was not affected by treatment with aspartame. The cell membrane of the control rabbit was more clearly visible than that of the rabbits in the treatment group, staining light blue in colour.

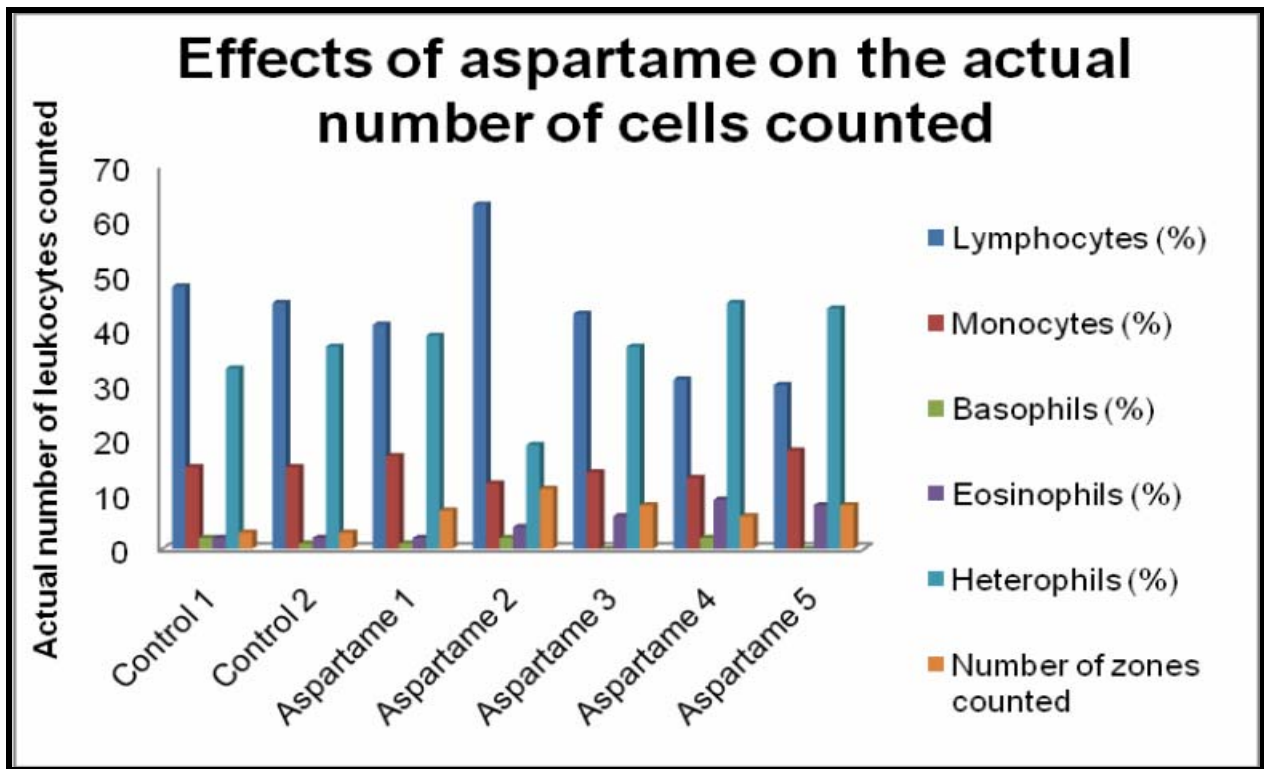
### ***7.3.2 Light microscopic study of the number of leukocytes***

After counting 100 leukocytes on each blood smear, the amount of each different leukocyte counted were expressed as a percentage of the 100 cells. These percentages are noted in Table 7.1. The table also indicates the number of zones that were counted to reach the 100 leukocytes.

**Table 7.1:** Number of leukocytes counted up to a 100 for each group, expressed as a percentage of that 100 leukocytes counted

<b>Rabbits</b>	<b>Lympho- cytes (%)</b>	<b>Monocytes (%)</b>	<b>Baso- phils (%)</b>	<b>Eosino- phils (%)</b>	<b>Hetero- cytes (%)</b>	<b>Number of zones counted</b>
<b>Control 1</b>	48	15	2	2	33	3
<b>Control 2</b>	45	15	1	2	37	3
<b>Aspartame 1</b>	41	17	1	2	39	7
<b>Aspartame 2</b>	63	12	2	4	19	11
<b>Aspartame 3</b>	43	14	0	6	37	8
<b>Aspartame 4</b>	31	13	2	9	45	6
<b>Aspartame 5</b>	30	18	0	8	44	8

**Graph 7.1:** The number of actual leukocytes counted for both the control and aspartame treated rabbits

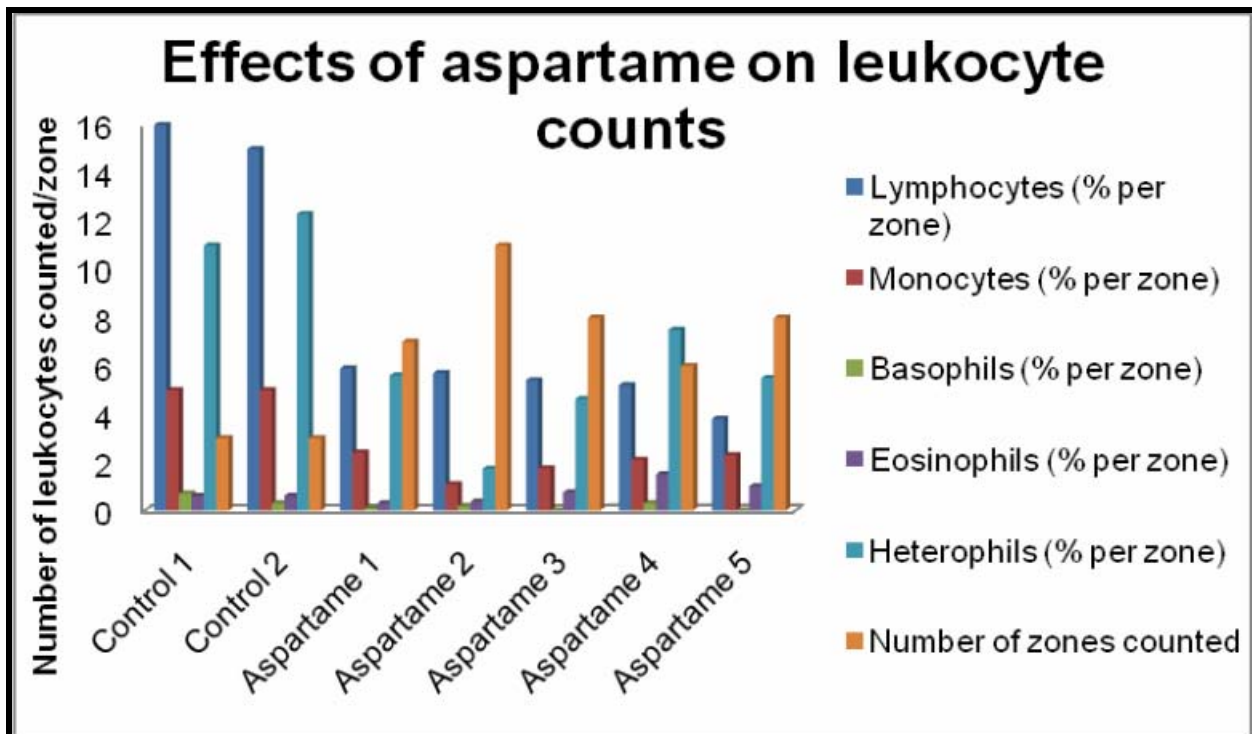


The number of zones was then used to determine the number of each specific leukocyte in each zone by dividing the total number of leukocytes counted through the number of zones counted (Table 7.2).

**Table 7.3:** Comparison between the number of leukocytes counted per zone for the control and aspartame treated rabbits

<b>Rabbits</b>	<b>Lympho- cytes (% per zone)</b>	<b>Monocytes (% per zone)</b>	<b>Basophils (% per zone)</b>	<b>Eosinophils (% per zone)</b>	<b>Heterophils (% per zone)</b>	<b>Number of zones counted</b>
<b>Control 1</b>	16	5	0.7	0.6	11	3
<b>Control 2</b>	15	5	0.3	0.6	12.3	3
<b>Aspartame 1</b>	5.9	2.4	0.1	0.3	5.6	7
<b>Aspartame 2</b>	5.7	1.09	0.18	0.36	1.73	11
<b>Aspartame 3</b>	5.4	1.75	0	0.75	4.63	8
<b>Aspartame 4</b>	5.2	2.1	0.3	1.5	7.5	6
<b>Aspartame 5</b>	3.8	2.3	0	1	5.5	8

**Graph 7.2:** Different leukocyte counts for the number of zones counted in both the control and aspartame treated groups



The number of zones counted in the controls was the same with small/no differences in the number of different leukocytes counted. The number of zones that was counted to obtain the 100 cells after treatment with aspartame increased from 3 to between 6-11 zones in the aspartame treated rabbits.

**Table 7.4:** Different leukocytes expressed as a percentage of the number of leukocytes in the control group

<b>Rabbits</b>	<b>Lymphocytes</b>	<b>Monocytes</b>	<b>Basophils</b>	<b>Eosinophils</b>	<b>Heterophils</b>
<b>Mean of controls</b>	15.5	5	0.5	0.6	11.65
<b>Mean of aspartame treated rabbits</b>	5.2	1.928	0.116	0.782	4.992
<b>Percentage of cells after treatment</b>	33.55	38.56	23.2	130.33	42.85

The number of lymphocytes obtained after treatment with aspartame decreased with 33.5% of that found in the control. A decrease in the number of cells were found and monocytes decreased by 38.52%, basophils by 23.2%, and heterophils by 42.85%. The eosinophils however increased by 30.33% if compared to the number of eosinophils counted in the control groups.

### **7.3.3 SEM study of the endothelial cells of the aorta**

Figure 7.6a and 7.6b illustrate the endothelial lining of a control rabbit.



**Figure 7.6a:** Endothelial lining of the control rabbit. White arrows indicate some of the many microvilli of the aorta (x550 magnification)

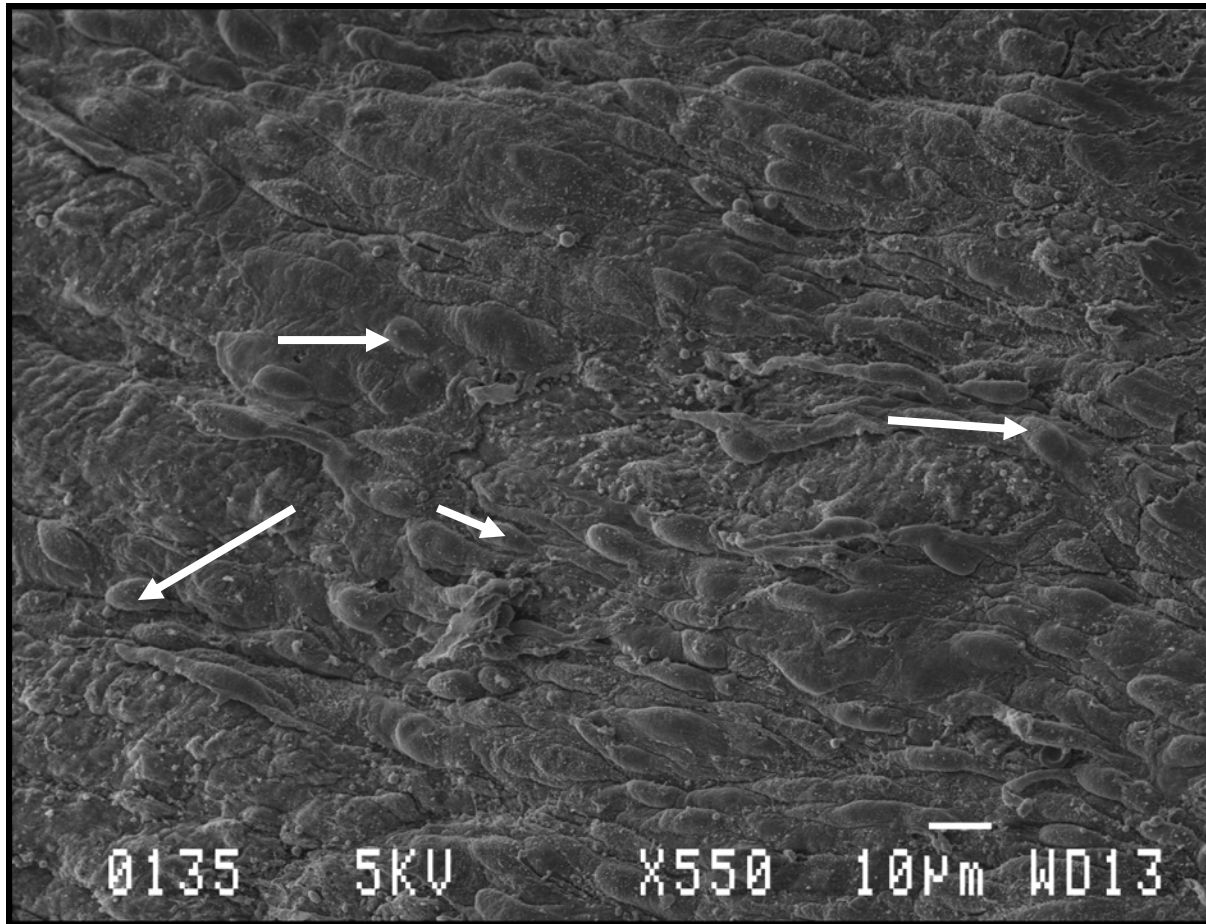


**Figure 7.6b:** Endothelial lining of the control rabbit (x500 magnification)

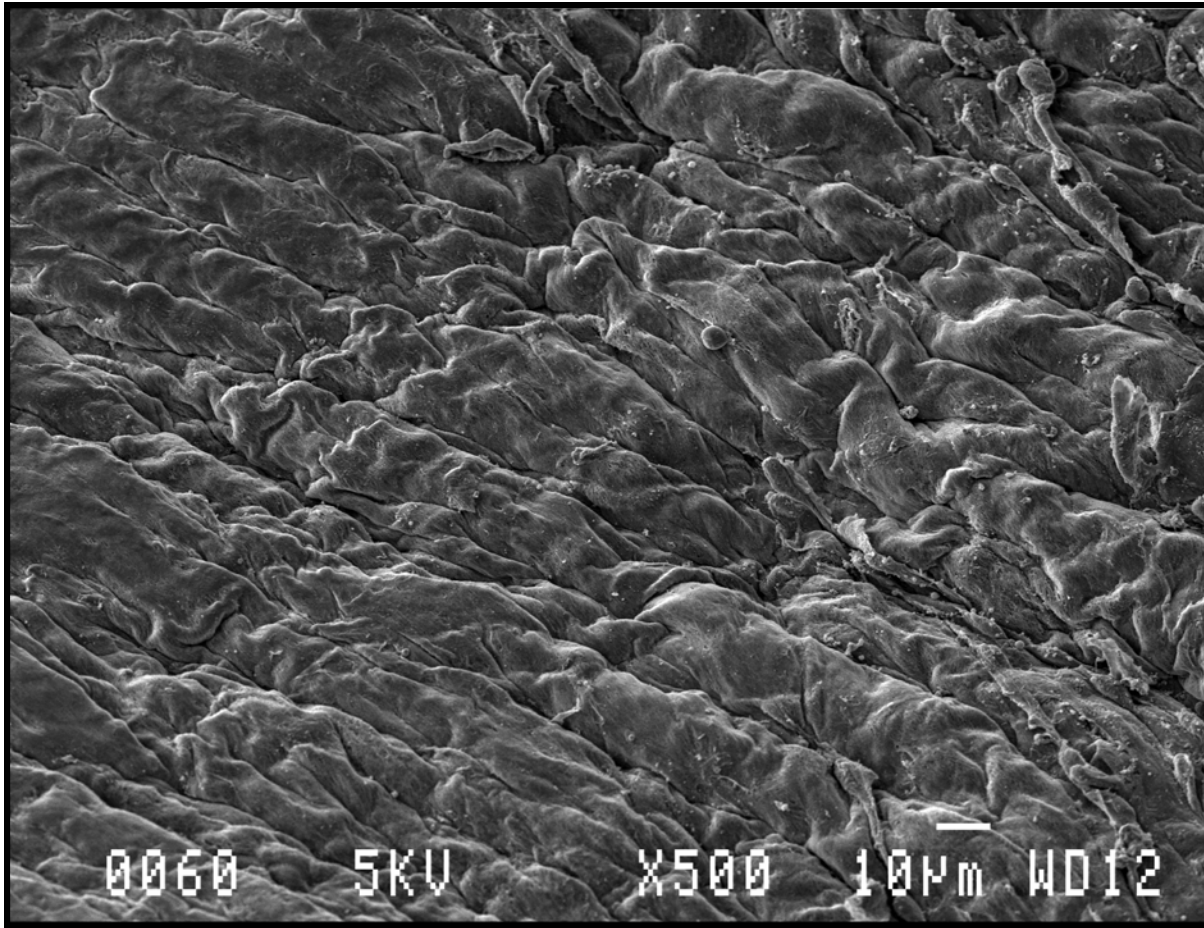


Figure 7.7 illustrates the endothelial lining of the control rabbit at an even higher magnification (x 3 500 magnification)

**Figure 7.7:** Smooth surface of the endothelial lining of a control rabbit. Circle indicate small microvilli of the aorta (x 3 500 magnification)

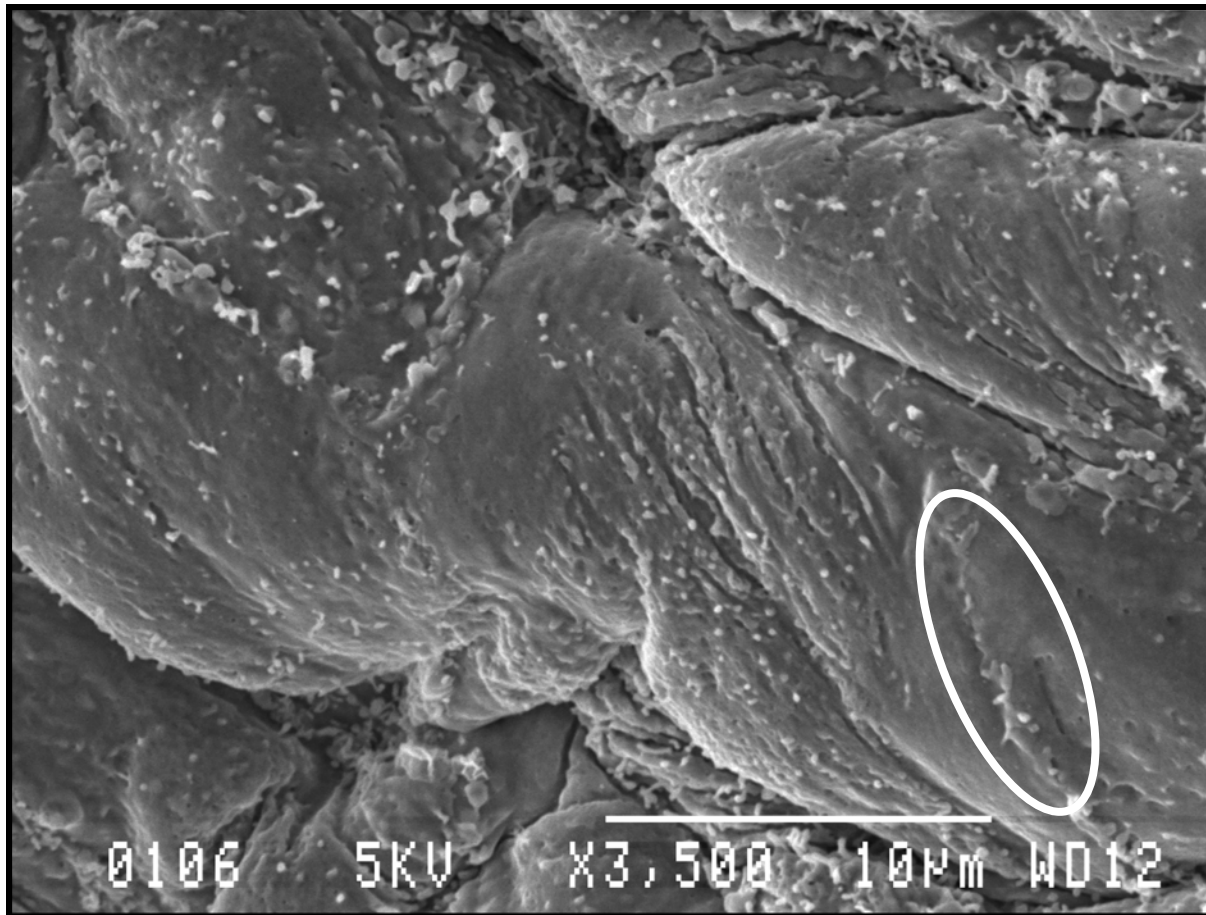


Figure 7.8 illustrates the endothelial lining of the rabbits after treatment with aspartame.

**Figure 7.8:** Endothelial lining of a rabbit after treatment with aspartame (x550 magnification)

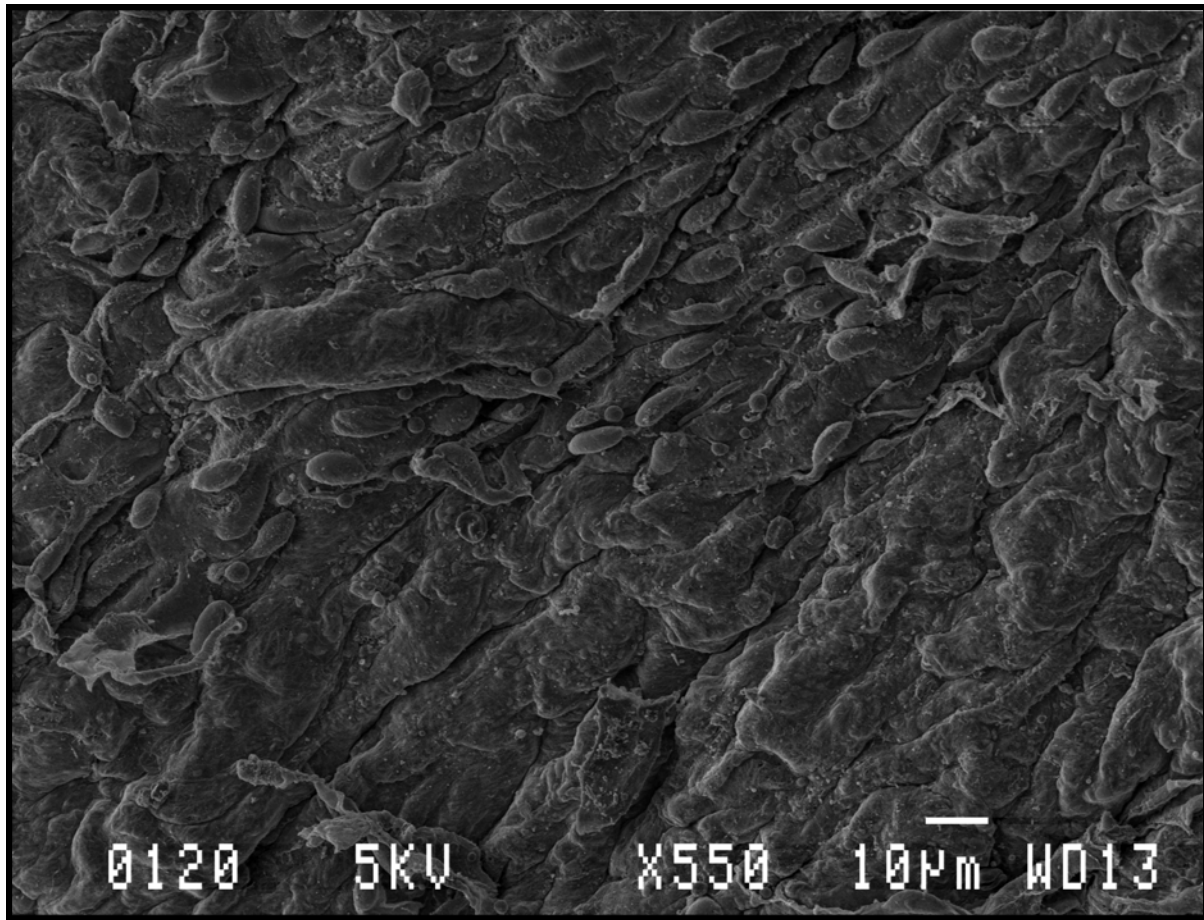
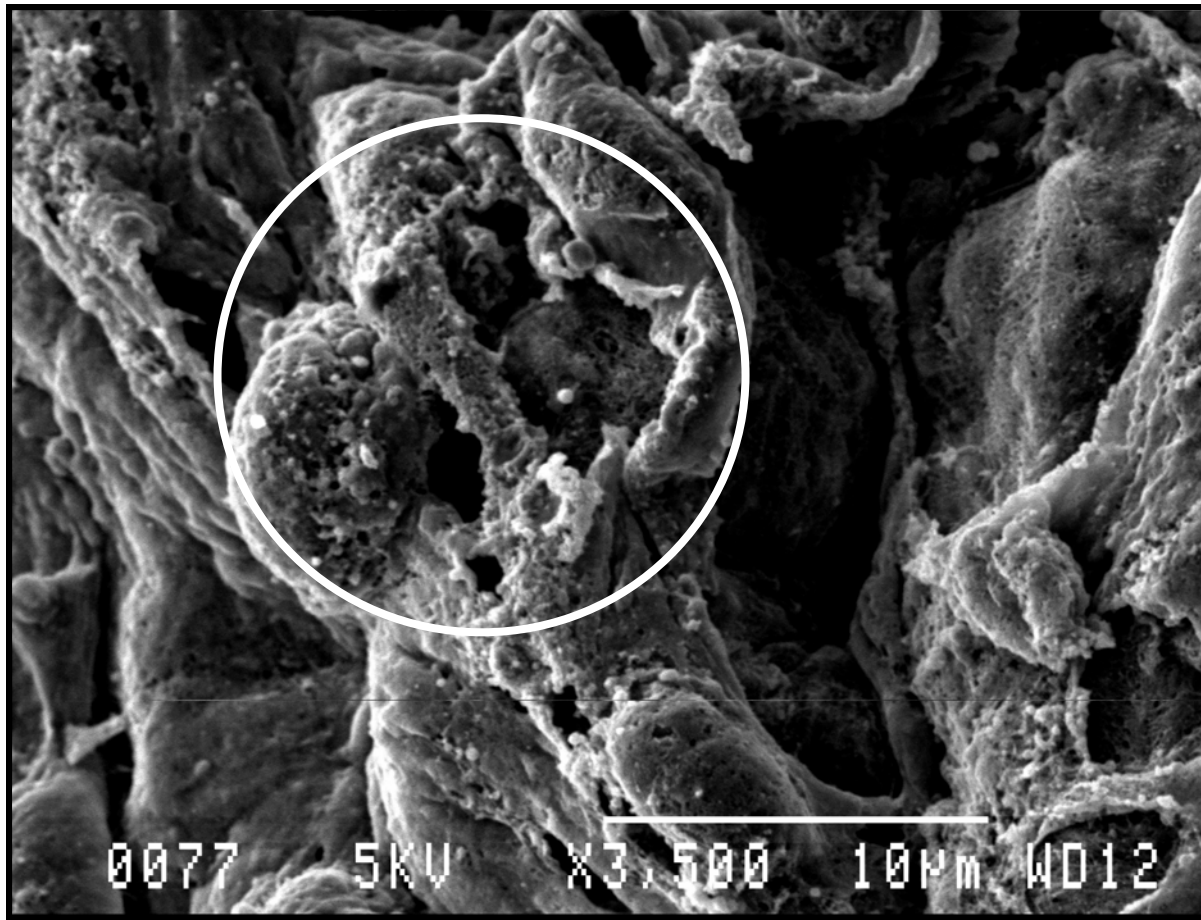


Figure 7.9a and 7.9b illustrates the endothelial lining of the same rabbit as in figure 7.8, only at x3 500 magnification.

**Figure 7.9a:** Endothelial lining of a rabbit after treatment with aspartame. Note the damage to the microvilli indicated by the circle (x3 500 magnification)



**Figure 7.9b:** Endothelial lining of a rabbit treated with aspartame. Arrows indicate filament fibers of the cytoskeleton. Note how contents of cell were spilling to outwards (x3 500 magnification)

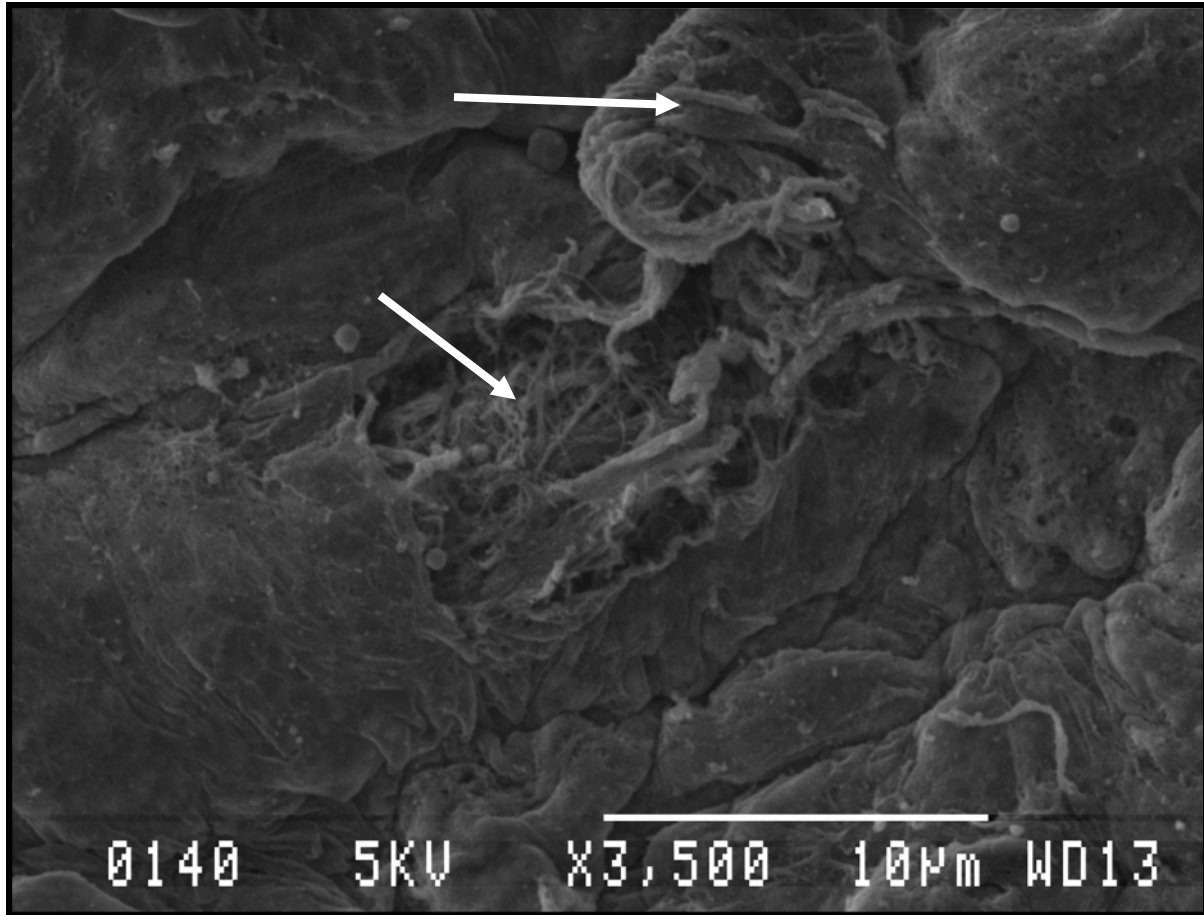


Figure 7.10 illustrates the effects of aspartame on the endothelial lining of a different rabbit after treatment.

**Figure 7.20:** Endothelial lining of a different rabbit after treatment with aspartame (x 550 magnification)

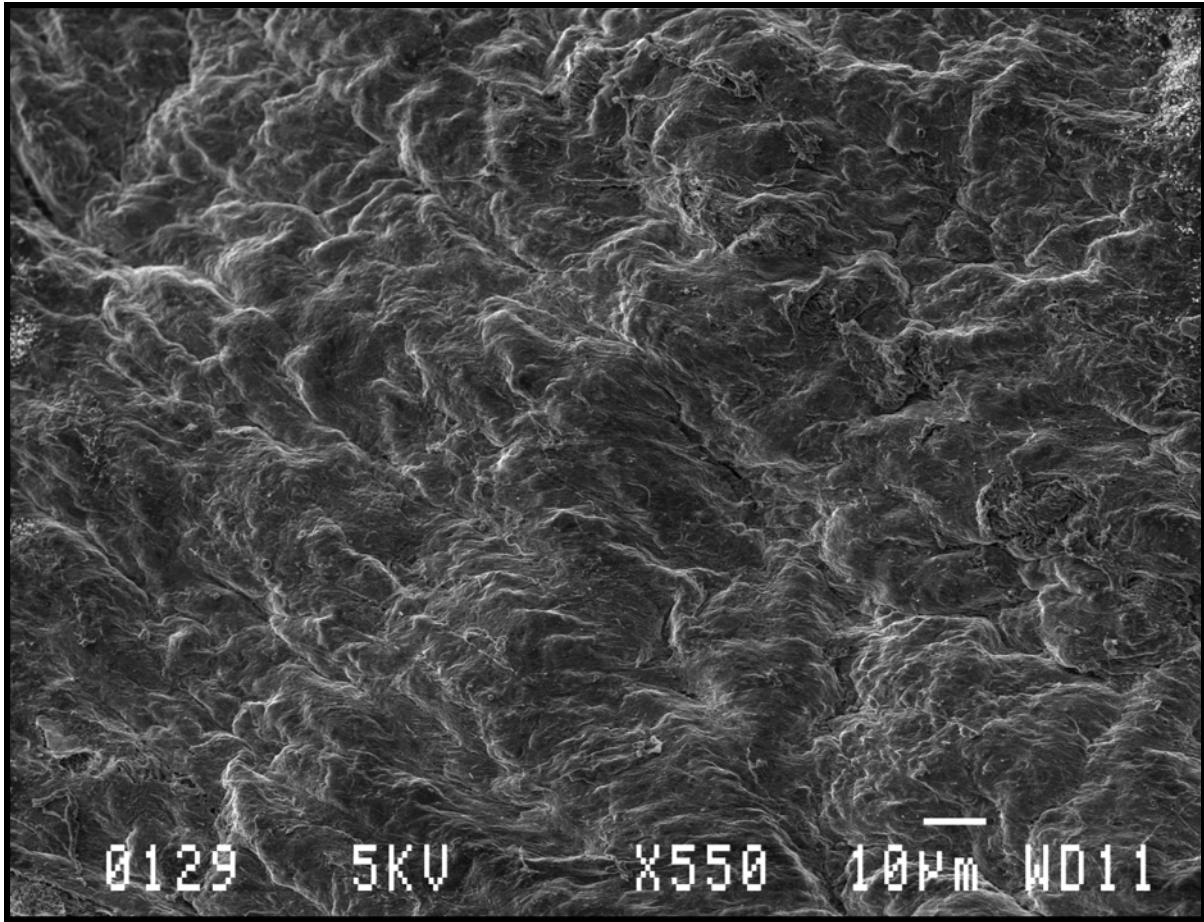


Figure 7.11 illustrates the endothelium in figure 7.10 at a higher magnification.

**Figure 7.11** Endothelial lining of a rabbit after treatment with aspartame. The white arrows indicate the filament fibers of the cytoskeleton (x3 500 magnification)

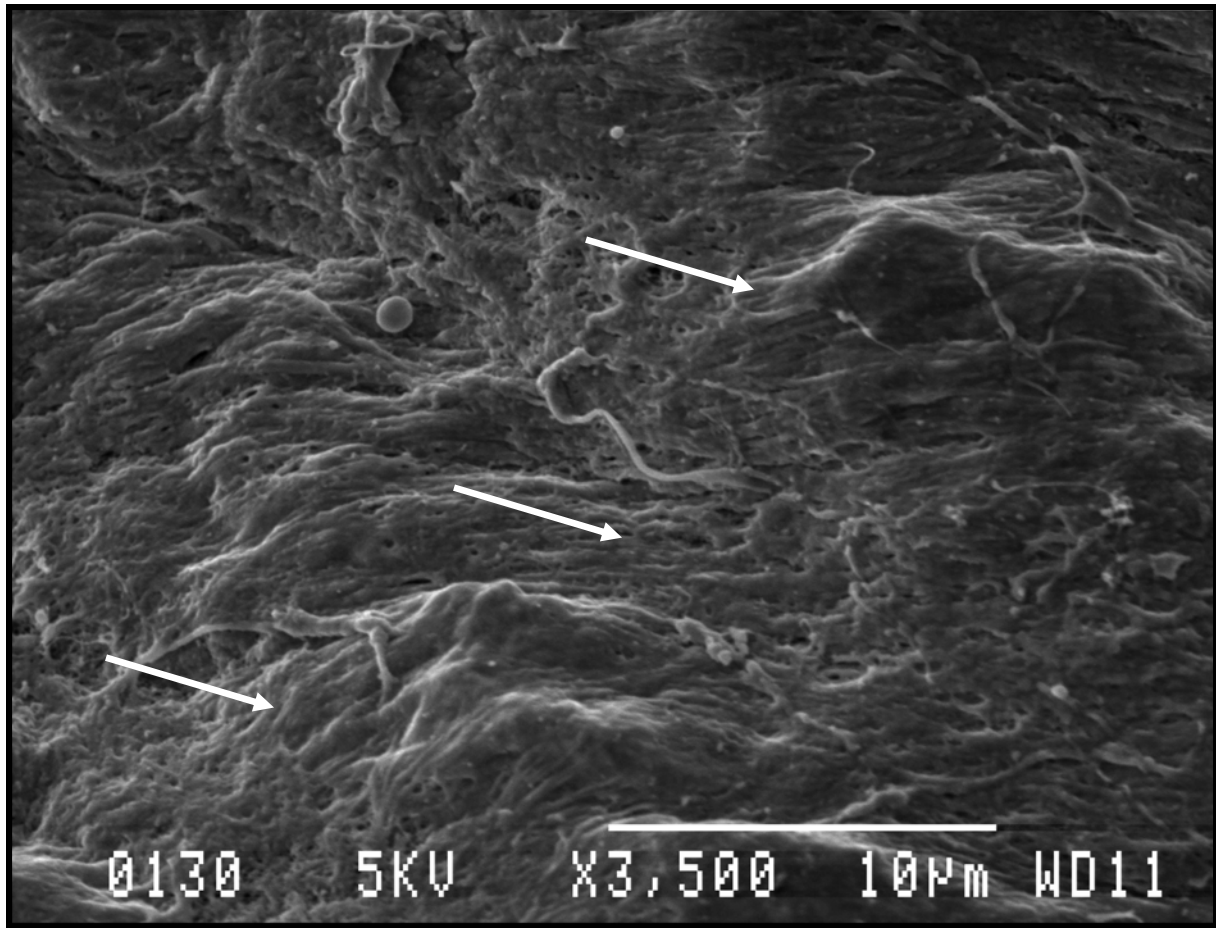




Figure 7.6a indicates the endothelial lining of the control rabbit, with the arrows indicating the microvilli found in the aorta. Fujimoto and co-workers in their study in 2005 also reported on finding endothelial microvilli in the aorta of the rabbit, particularly at the presumed site of foetal origin of the ductus arteriosus and near the origin of the subclavian artery. The samples of the aorta for this study were also taken from the area surrounding the origin of the subclavian artery. Figure 6b demonstrated normal endothelial morphology. The different endothelial cells could be distinguished with the cells exhibiting a long, elongated shape. The endothelial cells had a squamous, tile-like organization. At a higher magnification (Figure 7.7), the cell membrane had a smooth appearance. The oval indicates small hair-like projections (microvilli) from the cell membrane.

Figure 7.8 illustrates the microvilli of the endothelial lining of a rabbit treated with aspartame. At this lower magnification (x550) it seemed as though the treatment with aspartame had no adverse effect on the endothelial lining or the microvilli. When looking at this same endothelial lining at a higher magnification (x3 500) it is suggested that the aspartame did indeed adversely affect the lining, but it was only visible at a higher magnification. The microvilli of the aorta was damaged (Figure 7.9a) with holes appearing over the length of the microvilli. The membranes also appeared more porous with cytoskeleton being visible (inside circle). At a different area it also appeared as though the contents of the cell was spilling outwards (Figure 7.9b), and also here the cytoskeleton was visible, as indicated by the arrows.

Figures 7.10 and 7.11 illustrated the endothelial lining of a different rabbit after treatment with aspartame. At the lower magnification (Figure 7.10) it would appear as though the endothelial lining formed a continuous layer and no individual cells could be distinguished. The higher magnification (Figure 7.11) revealed distinct filament-like structures, as appose to the control (Figure 7.6b) where clear endothelial cells with smooth cellular membranes could be distinguished with microvilli in areas closely related to the origin of the subclavian artery (Figure 7.6a).

#### 7.3.4 TEM study of the endothelial cells of the aorta

Figures 7.12a and 7.12b illustrate the nuclei of endothelial cells of a control rabbit.

**Figure 7.12a:** Illustration of the nucleus of an endothelial cell of a control rabbit. Note the clear nuclear envelope (arrow) and the even distribution of the chromatin throughout the nucleus (white arrow) (x7 500 magnification)

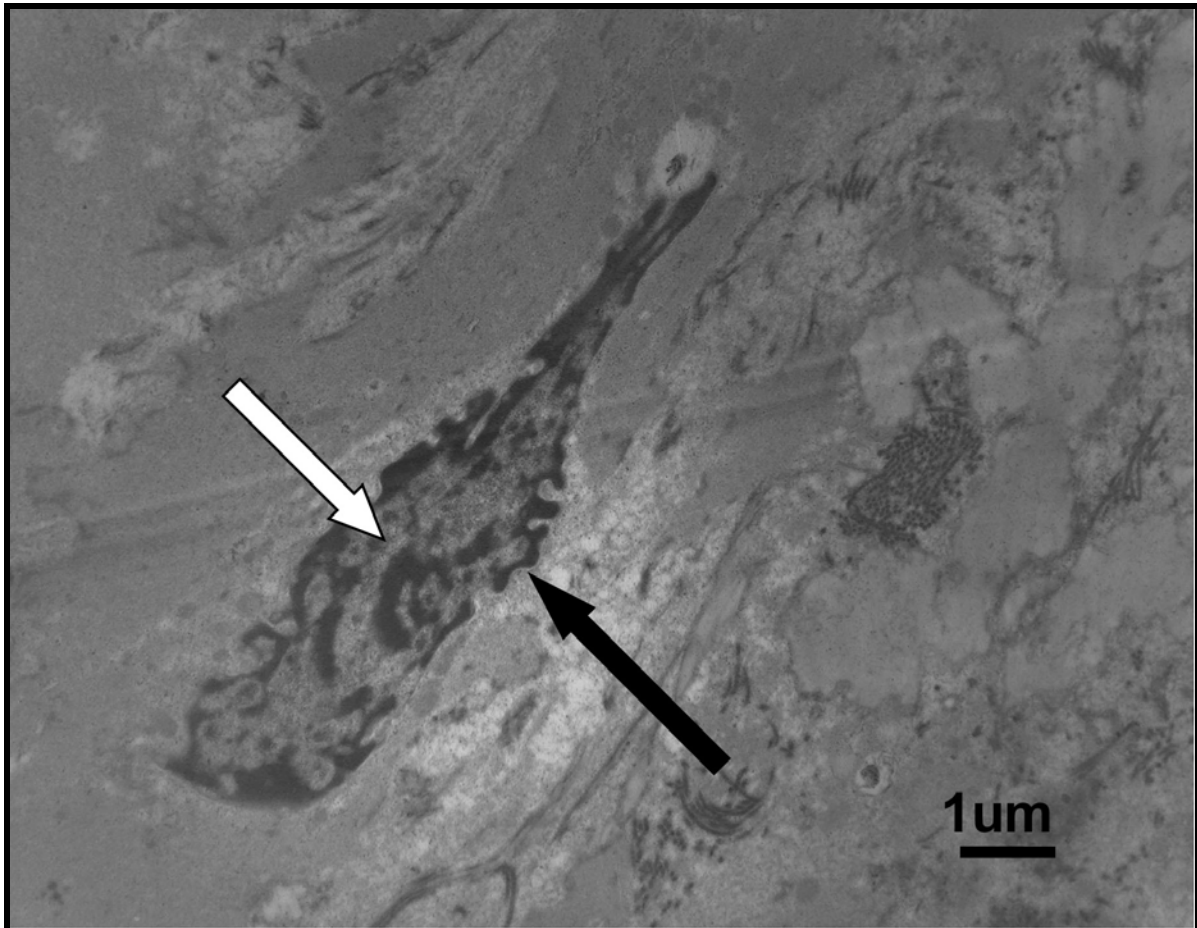


**Figure 7.12b:** Illustration of the nucleus of an endothelial cell of a control rabbit. Note the clear nuclear envelope (arrow), the nucleolus (white arrow) and the cytoplasm of another endothelial cell (dashed arrow) with a tight junction being visible just to the right of it (x7 500 magnification)

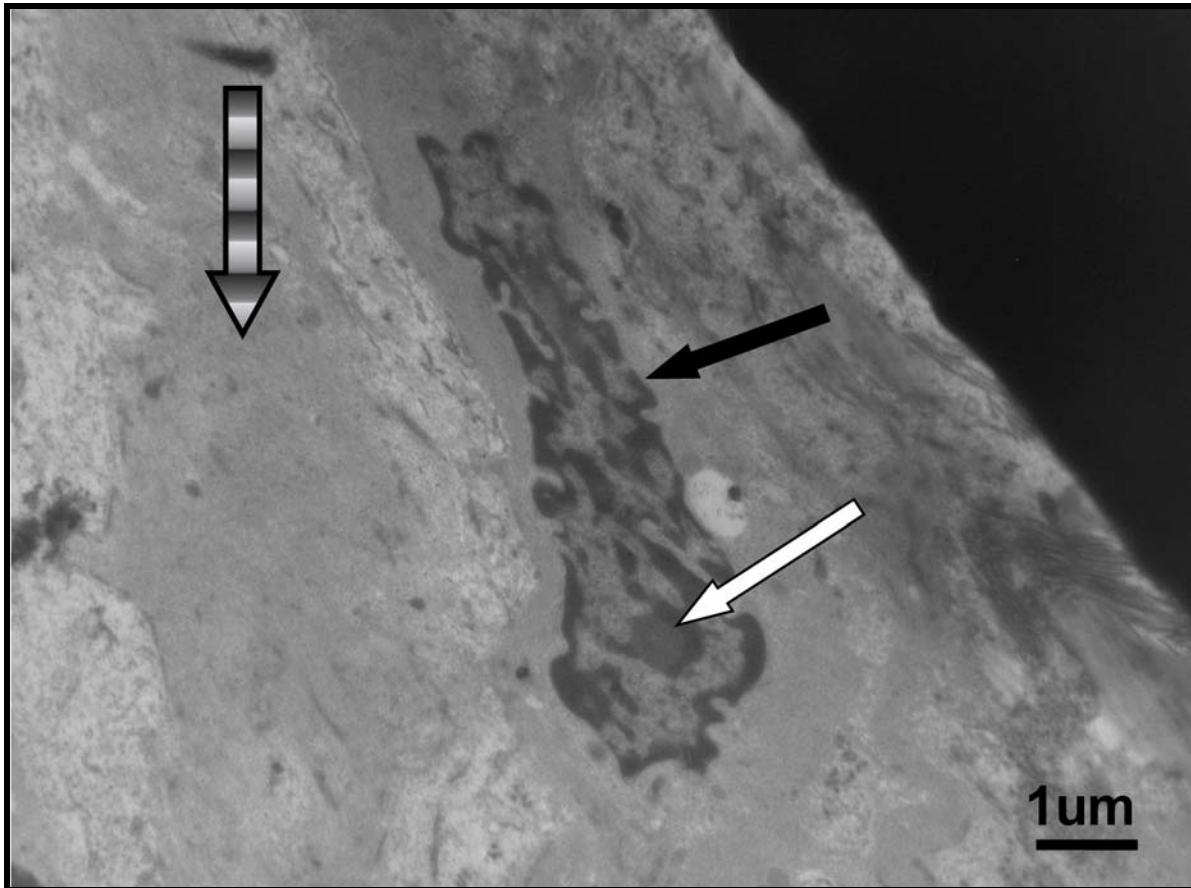
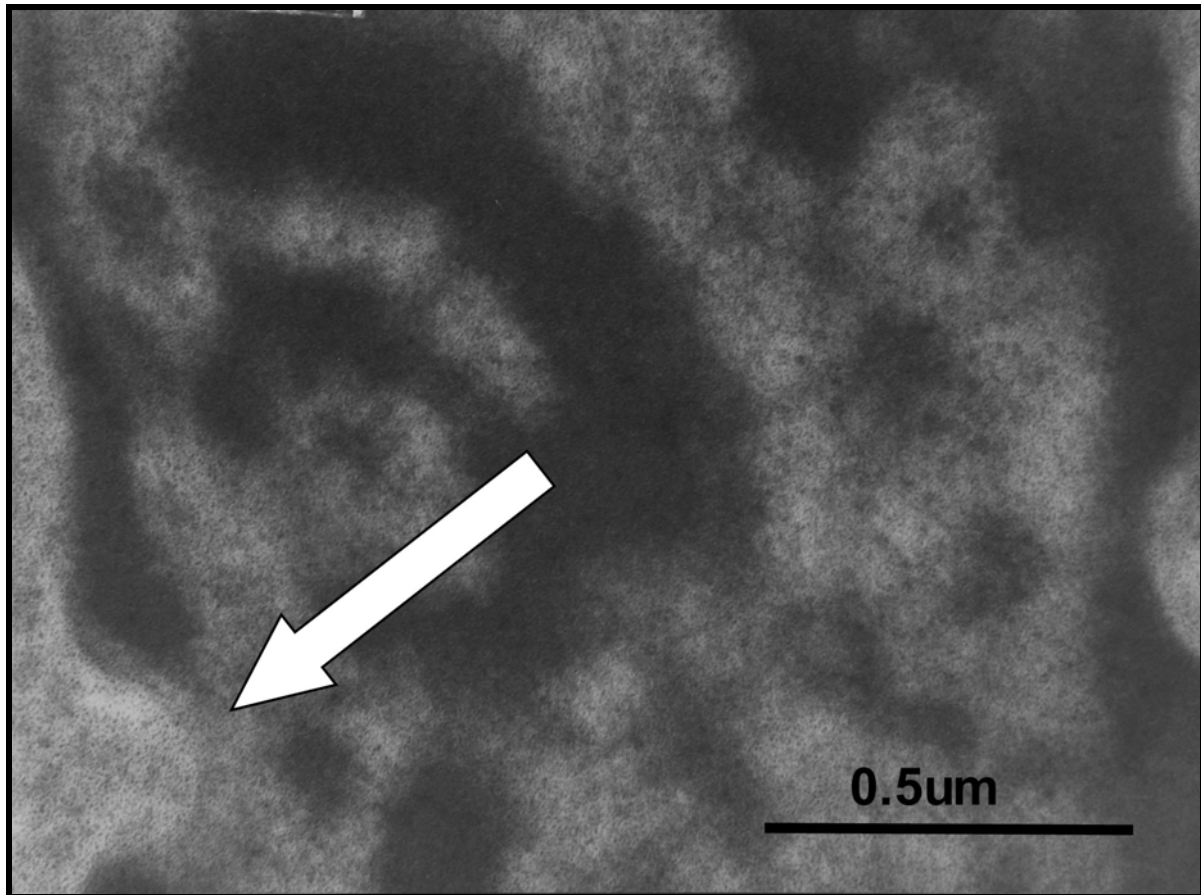


Figure 13 illustrates the nuclear envelope and chromatin of an endothelial cell of a control rabbit.

**Figure 7.13:** The chromatin of an endothelial cell of a control rabbit. Note the clear nuclear envelope (white arrow) and the even distribution of the chromatin (x59 000 magnification)



Figures 7.14a and 7.14b illustrates the nuclei of endothelial cells of a rabbit after treatment with aspartame.

**Figure 7.14a:** Illustration of the nucleus of an endothelial cell of a rabbit after treatment with aspartame. Note the fact that the nuclear envelope is visible on some areas (arrow), and absent in other (dashed arrow). The chromatin visibly underwent nuclear envelope marginalization (white arrows) (x7 500 magnification)

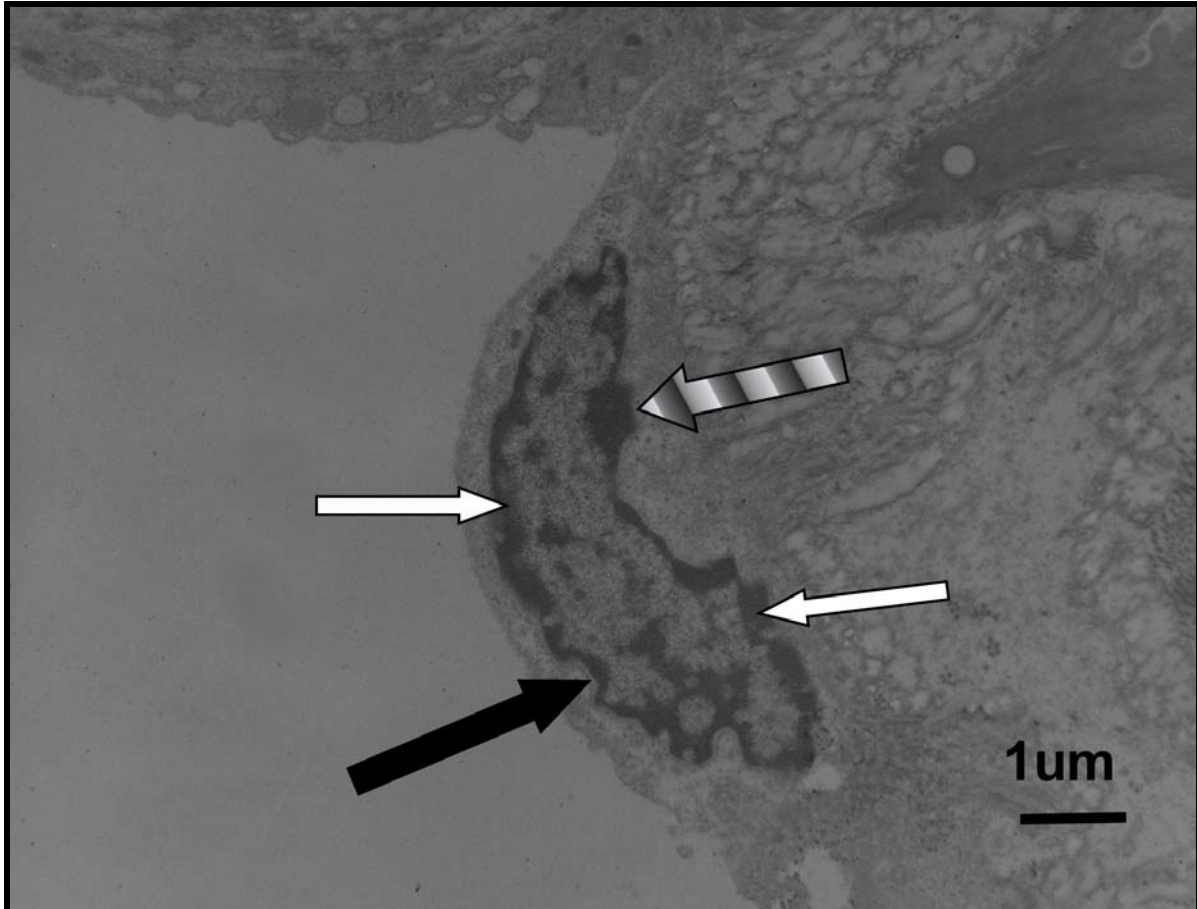


**Figure 7.14b:** Illustration of the nucleus of an endothelial cell of a rabbit after treatment with aspartame. Note the nuclear envelope marginalization of the chromatin (white arrows), with nuclear envelope being visible in some areas (arrow) and absent in other areas (dashed arrow). Also it appears as though some of the chromatin was spilling from the nucleus into the cytoplasm (dashed arrow). Rupture of the cellular membrane was clearly visible (circle) (x7 500 magnification)

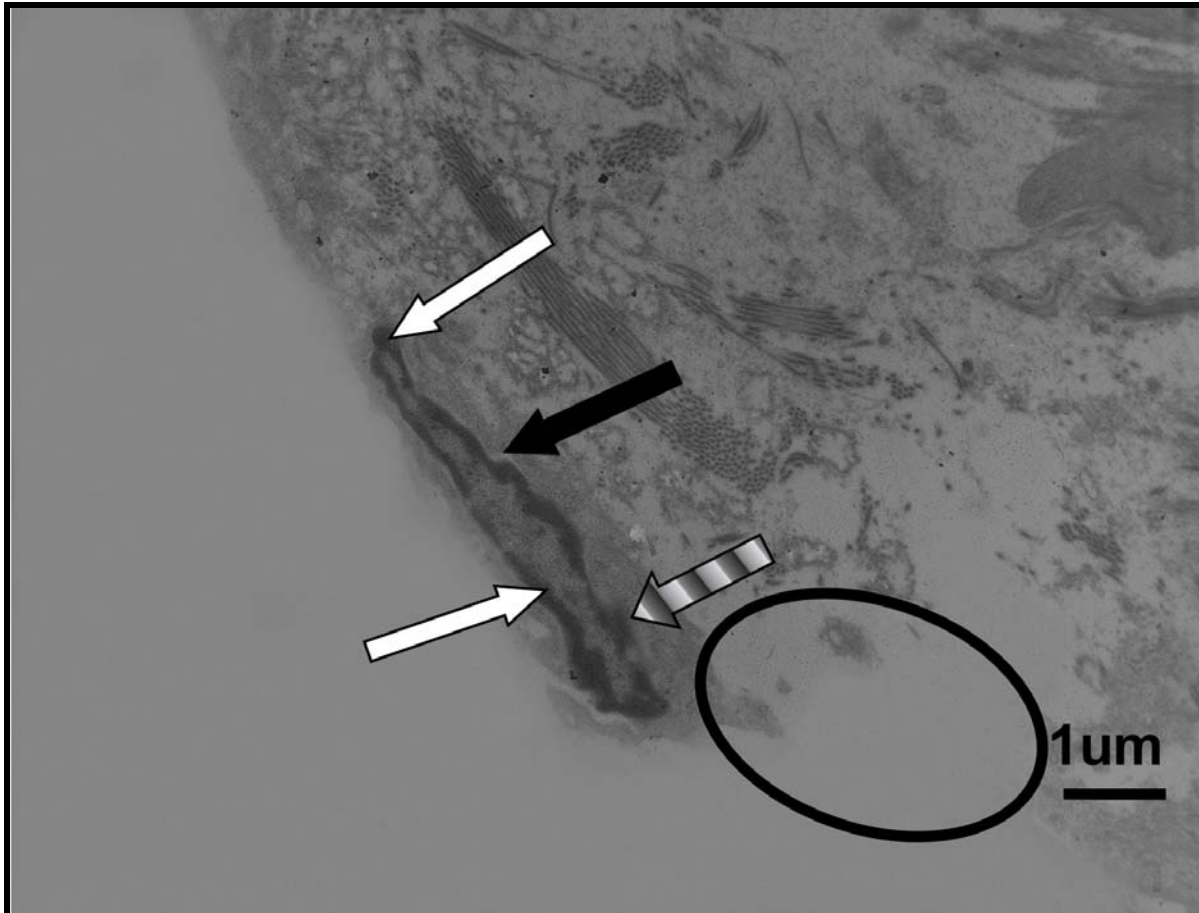
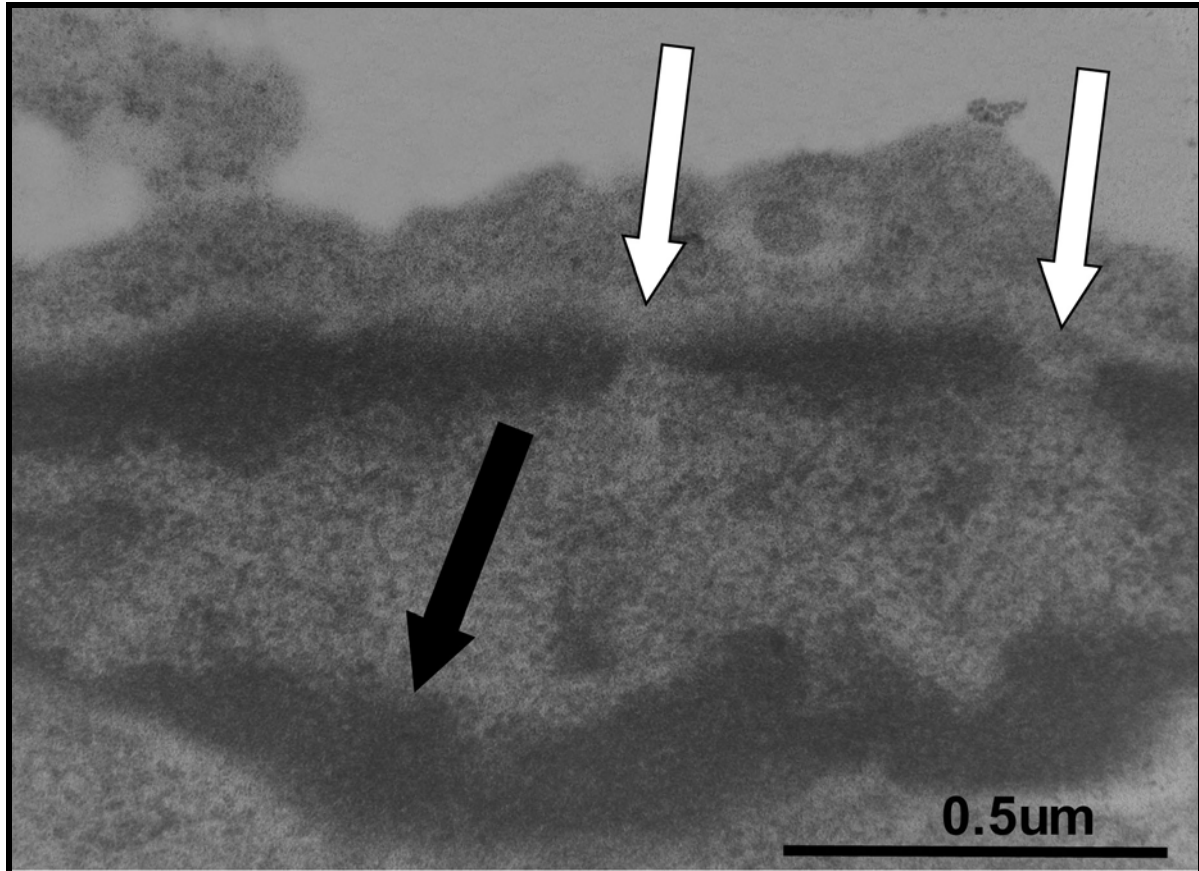


Figure 7.15 illustrates the nucleus of an endothelial cell at a higher magnification.

**Figure 7.15:** The chromatin inside the nucleus of an endothelial cell of a rabbit after treatment with aspartame. Chromatin marginalization towards the nuclear envelope was clearly visible (arrow), with little to no chromatin towards the centre of the nucleus. The nuclear envelope was also not clearly distinguishable. Damaged areas of the nuclear envelope was visible at two areas (white arrows) (x59 000 magnification)



Figures 7.12a and 7.12b illustrated the nucleus of an endothelial cell of a control rabbit. The nuclear envelope was clearly visible in both illustrations with the chromatin of the nuclei being evenly distributed. The nucleolus of the nucleus and the cell membrane of the endothelial cell were also easily distinguishable in figure 7.12b. At a higher magnification (Figure 7.13) the chromatin of the endothelial cell was clearly visible and evenly distributed. The nuclear envelope could also be distinguished, with no apparent damage.

Figure 7.14a illustrated an endothelial cell of a rabbit after treatment with aspartame. The nucleus was clearly visible, with the chromatin appearing condensed and marginalized towards the nuclear envelope. Little to no chromatin was visible in the centre of the nucleus. The nuclear envelope was visible in certain areas and absent in others. Damage to the cellular membrane of the endothelial cell was clearly visible in figure 7.14b with the contents of the cytoplasm appearing to spill outwards. The chromatin of the nucleus of this endothelial cell, obtain from a rabbit fed aspartame, also demonstrated the nuclear envelope marginalization of the chromatin. It appeared as though some of the chromatin was spilling into the cytoplasm in an area where the nuclear envelope was not visible. The nuclei of these endothelial cells also appeared smaller than those of the control (Figures 7.12a and 7.12b). At a higher magnification of the nucleus of an endothelial cell after treatment with aspartame (Figure 7.15), the nuclear envelope marginalization was clearly visible with possible areas of damage to the nuclear envelope. The chromatin was also not evenly distributed through the whole of the nucleus.

## **7.4 SUMMARY AND EXPLANATION**

### **7.4.1 Light microscopic studies of the morphology of the leukocytes and the number of different leukocytes counted**

Photos were taken of the different leucocytes to compare possible morphological differences between the controls and aspartame treated rabbits. The results obtained for the control leukocytes can be summarized as per table 7.4.



**Table 7.5:** Comparison between the morphology of the leukocytes of the control and aspartame treated groups

<b>Cells</b>	<b>Nuclei and chromatin</b>	<b>Cytoplasm</b>	<b>Granules</b>	<b>Cell membrane</b>
<b>Lymphocytes</b>	<b>Controls</b>	Stained dark blue with the chromatin more densely packed	None	Visible
	<b>Aspartame</b>	Stained lighter blue		
<b>Monocytes</b>	<b>Control</b>	Stained dark blue with chromatin densely packed	None	Visible
	<b>Aspartame</b>	Stained dark blue and was bean-shaped		
<b>Basophils</b>	Bi-lobar	Control stained a deeper blue than aspartame rabbit	Dark blue	More clearly visible

**Table 7.4 (continue):** Comparison between the morphology of the leukocytes of the control and aspartame treated groups

<b>Cells</b>	<b>Nuclei and chromatin</b>	<b>Cytoplasm</b>	<b>Granules</b>	<b>Cell membrane</b>
<b>Eosinophils</b>	Bi-lobar with distinct dark blue stain	Red	Red granules visible	More clearly visible in the control
<b>Aspartame</b>	Chromatin more densely packed closer to nuclear envelope		Stained more brilliantly	
<b>Heterophils</b>	Brilliantly blue with up to 5 lobes visible		Red granules, stained more brilliantly in control; individual granules visible in control	More clearly visible in control, staining light blue
	Chromatin of aspartame treated rabbit more densely packed		Red granules less in aspartame rabbits and not as clearly distinguishable	

It would appear as though aspartame affected some of the morphology of the different leucocytes, but the size of the cells were not adversely affected. The cytoplasm of the basophils of the aspartame treated rabbit did not stain as dark blue as that of the control, which could be an indication that the number of granules (secrete heparin and histamine) inside the cytoplasm decreased. Heparin, binds to enzyme inhibitor antithrombin III (AT III) leading to conformational change which result in its active site being exposed. The activated AT III then inactivates thrombin and other proteases involved in blood clotting, most notably factor Xa. The rate of inactivation of these proteases by AT III increases 1000-fold due to the binding of

heparin (Bjork and Lindahl, 1982). From results obtained in chapter 5 regarding the coagulation profile of the rabbits after treatment with aspartame, it was concluded that the amount of thrombin decreased leading to bleeding tendencies. Heparin assist in the process of thrombin inhibition, thus it is hypothesized that an immune response was triggered and that the number of granules inside the basophils decreased in order for less heparin to be secreted which would further increase the inability for coagulation.

The granules of the eosinophils of the aspartame treated rabbits, on the other had, stained more brilliantly red which leads to the hypothesis that the number of granules increased after treatment with aspartame. Eosinophils are known to modulate allergic reactions by secreting the substances in their granules which neutralize histamine and inhibits degranulation of mast cells (contain heparin and histamine) (Meyer and Meij, 1996). It was also shown, in table 7.3, that the number of eosinophils increased by 30.33% when compared to counts obtained for the controls. Thus, it is hypothesized that the increase in the amount of eosinophils and thus also the amount of granules (due to increase in number of eosinophils and as seen in figure 7.4b) were due to an immune response to correct the decrease in coagulation, caused directly by the decrease in the concentration of factors VII, X and VIII after treatment with aspartame as discussed in chapter 5 of this thesis.

The number of granules in the heterophils of the aspartame treated rabbits appeared less and they were not as clearly distinguishable as compared to that of the controls. The granules inside the heterophils are known to be lysozymes and phagocytin, two antibacterial agents (Archer *et al.*, 1963). Results also indicated (Table 7.3) that the number of heterophils decreased by 42.85% when compared to numbers obtained for the control rabbits. Thus, when taking into account that the number of cells and granules or levels of antibacterial agents in the granules appeared to decrease (less brilliant staining of the granules in cytoplasm), the ability of the cells to protect against bacterial infection would decrease. Thus it is hypothesized that the rabbits might have suffered from a degree of suppressed immunity and that bacterial infections could occur more easily (due to lower number of heterophils and granules inside cytoplasm).

The increase in the number of zones that had to be counted to obtain the 100 leukocytes in the aspartame treated rabbits reflects that the total number of leukocytes decreased. This could be an indication that the rabbits suffered from a degree of suppressed immunity. The number of eosinophils, however, increased as an immune defence mechanism to prevent further inability for coagulation.

#### **7.4.2 SEM study of the endothelial lining of the aorta**

The tendency of blood to coagulate intravascularly is prevented by a number of mechanisms and any coagulate that does form will be dissolved in time. Intravascular coagulation is prevented by the following:

- The smooth endothelial lining of the cardiovascular system;
- The continuous circulation of blood;
- Prostacyclins (produced by endothelial cells) that prevent platelet aggregation;
- Anti-thrombin III – circulating factor that binds to thrombin, inactivating it;
- Heparin, a natural anti-coagulant which is secreted by mast cells and basophils (Guyton and Hall, 2006) – improves inactivation of thrombin by antithrombins. (Meyer and Meij, 1996).

The results obtained in this study indicate that the endothelial lining of the aorta was damaged after treatment with aspartame. The microvilli present in the aorta were also damaged (Figure 7.9a) and it appeared as though the cellular contents were spilling outwards (Figure 7.9b) with the cytoskeleton also being visible. Another, but similar picture was painted by figure 7.10 that illustrated that no individual endothelial cells were visible. Filament-like structures were visible on the higher magnification (Figure 7.11), thus the cytoskeleton of the cells was exposed. The endothelial cell integrity was disrupted during treatment with aspartame, which made the aorta samples from the aspartame treated rabbit more prone to damage during the critical point drying procedure, disrupting the cellular membranes of the endothelial cells. This disruption of cell membranes were not observed in the control samples (Figure 7.6b and 7.7). As seen from above, endothelial cells play an important role in maintaining haemostasis in the vascular system, thus damage to the endothelial cells could lead to an increased amount of coagulation. The endothelial cells are also responsible for the synthesis and release of F VIII into the blood stream (Rubin and Leopold, 1998). Thus, it is hypothesized that the decrease in the

concentration of circulating F VIII, as described in chapter 4 of this thesis could be due to the extend of the damage to the endothelial cells (Figures 7.9a, 7.9b and 7.11).

#### **7.4.3 TEM study of the endothelial lining of the aorta**

Results obtained during further ultra-structural analysis of the endothelial cells with the TEM confirmed results obtained by the SEM. Damage to the nucleus was clearly visible, with regards to the distribution of the chromatin (marginalization towards the nuclear envelope) and damage to the nuclear envelope itself (not visible in all areas). The cellular membrane of the endothelial cells was also damaged (Figure 7.14b), which confirms the results obtained on the SEM, also indicating cellular membrane damage (Figures 7.9a and 7.9b). The nuclei of the endothelial cells after treatment with aspartame also appeared smaller (Figures 7.14a and 7.14b).

Characterization of apoptosis mainly derives from morphological and ultra-structural observations (Kerr, Wyllie and Currie, 1972). Intracellular and plasma membrane structural modifications have been widely recognized as crucial factors involved in cell injury and cell death. Changes in nuclear morphology and in organelle structure as well as specific phenomena at the cell surface level, namely surface smoothing and surface blebbing, are often considered as markers associated with cell pathology (Allen, 1987). In addition, it must be recalled that these structural findings are intimately related to the cascade of biochemical and physiological events leading to changes in cellular homeostasis, to the loss of cell volume regulation, to some modifications of macromolecule synthesis and, finally the loss of cell viability (Malorni, Fais and Fiorentini, 1998). A single intracellular event can be extensively analysed by using, in parallel, biochemical, molecular or ultra-structural approaches. The complex sequence of structural modifications ultimately leading to cell death can be recognized by light and electron microscopy techniques. These analyses are mainly qualitative and can indicate: i) the different features of the apoptotic process in terms of appropriate markers, e.g. histo-type associated; and ii) the staging of the process, e.g. early or late phases (also called secondary necrosis). However, quantitative analysis, i.e. cytometric and morphometric, can also be performed by using light microscopy, fluorescence microscopy, confocal microscopy, SEM and in some conditions TEM (Bellomo *et al.*, 1994; Malorni *et al.*, 1993; Allen, 1997).

A cell undergoing apoptosis shows characteristic morphology that can be observed microscopically:

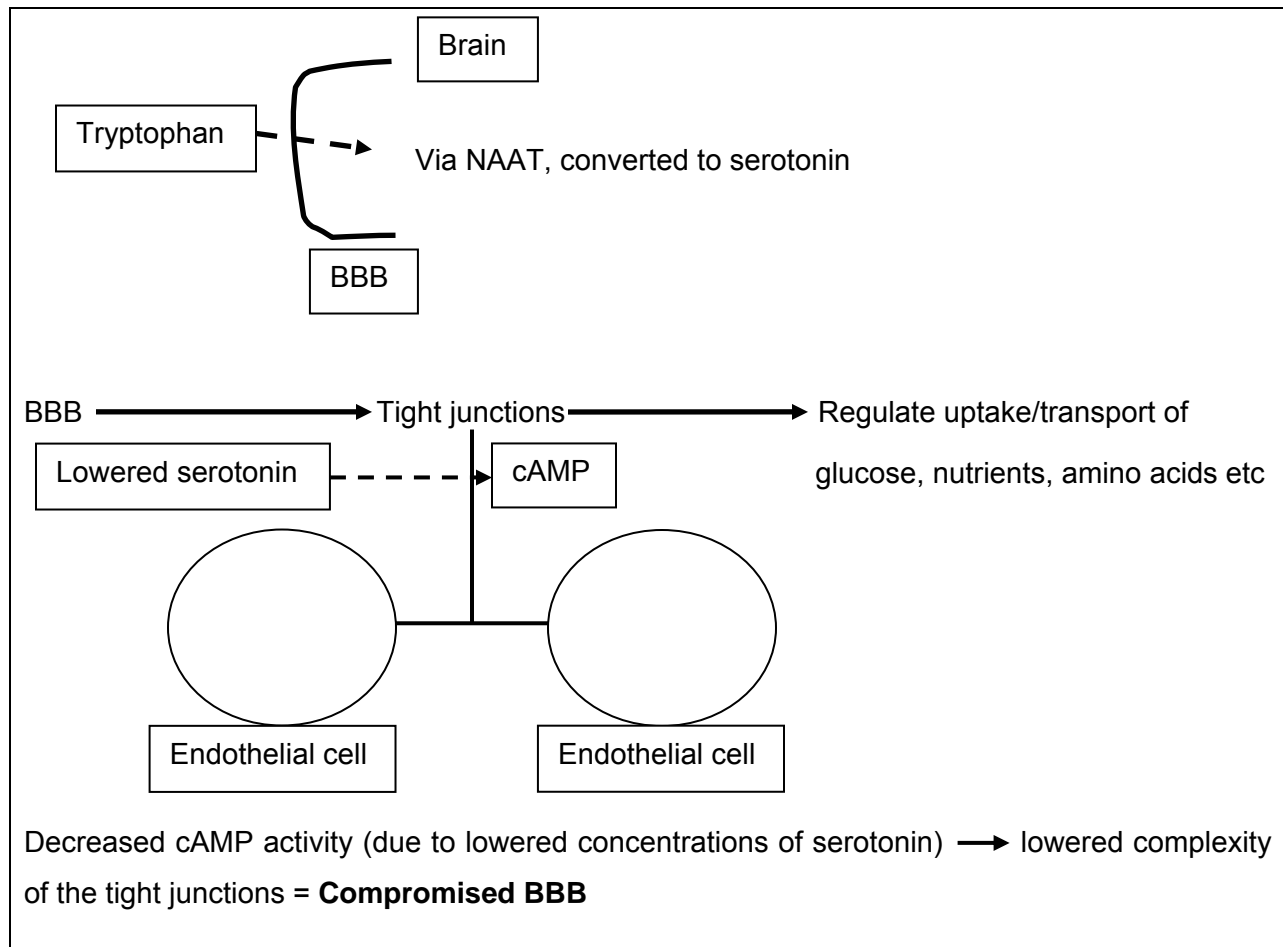
1. Cell shrinkage and rounding due to the breakdown of the protein-like skeleton by caspases
2. The cytoplasm appears dense, and the organelles appear tightly packed
3. Chromatin undergoes condensation into compact patches against the nuclear envelope in a process known as pyknosis, a hallmark of apoptosis
4. The nuclear envelope becomes discontinuous and the DNA inside it is fragmented in a process referred to as karyorrhexis. The nucleus breaks into several discrete chromatin bodies or nucleosomal units due to the degradation of DNA
5. The cell membrane shows irregular buds known as blebs
6. The cell breaks apart into several vesicles called apoptotic bodies, which are then phagocytosed (Susin *et al.*, 2000; Kihlmark, 2001; Nagata, 2000).

Thus, it could be summarized that the endothelial cells were experiencing cellular pathology as changes in their nuclear morphology (condensation and marginalization of chromatin; damage to nuclear envelope) and cell surface smoothing (Figure 7.10) were visible. Also, cell pathology leads to modifications in the synthesis of macromolecules. Thus the production and secretion of F VIII by the endothelial cells could have decreased, as proven by the results obtained in chapter 5. The two changes in the nuclear morphology is also hallmarks for apoptosis (bullets 3 and 4 mentioned above), thus it was clear that the endothelial cells were undergoing apoptosis.

Endothelial cells and their tight junctions form an integral part of the blood brain barrier (BBB) (Leeson, Leeson and Paparo, 1988). Phenylalanine, constituting 50% of the metabolites of aspartame, binds to a neutral amino acid transporter (NAAT) to be carried over the BBB. Other amino acids namely tryptophan, methionine, branched-chain amino acids and tyrosine, necessary for production of important neurotransmitters, also have to bind to the NAAT for transport over the BBB. Thus there is competition for NAAT to be carried over the BBB, so that the amino acids can be converted to their respective neurotransmitter counterparts.

Phenylalanine is also converted to tyrosine (precursor of DOPA and dopamine) by the enzyme phenylalanine hydroxylase in the liver. Thus, a certain amount of circulating phenylalanine will be converted to tyrosine, but a large amount of the phenylalanine will occupy the NAAT (due to larger concentrations in the blood after intake of aspartame with no synchronised administration of valine [Maher and Wurtman, 1987]), making it impossible for other amino acids to be carried over the BBB. Tryptophan, one of the amino acids necessary for the production of serotonin in the brain, also utilise the NAAT for transport. It has been proven that phenylalanine from aspartame decreases the concentration of serotonin produced due to the competition between phenylalanine and tryptophan for transport via NAAT over the BBB, with phenylalanine almost always occupying NAAT due to its high concentrations (Sharma and Coulumbe, 1987). Also it was shown in chapter 6 of this thesis that platelet aggregation was decreased (SEM), due to a direct decrease in the amount of circulating thrombin necessary for the degranulation of the platelets (dense granules contain serotonin, necessary for platelet-platelet aggregation), thus indirectly decreasing the amount of circulating serotonin. cAMP plays an integral part in the complexity of the tight junctions between the endothelial cells which form part of the BBB. A decreased concentration of circulating serotonin lowers the activity of cAMP, and decreased cAMP activity leads to a decrease in the complexity of the tight junctions between the endothelial cells (Humphries *et al.*, *In Press*). Thus, it is hypothesized that due to the lowered concentrations of serotonin present (decreased transport of tryptophan over BBB and decreased thrombin concentrations, as described above), the BBB was compromised as both the tight junctions could have been affected (lowered activity of cAMP due to decrease in concentration of circulating serotonin) and the apoptotic appearance of the endothelial cells (TEM).

**Diagram 7.1:** Effects of inability to convert tryptophan to serotonin on the cAMP activity



Adapted from Humphries *et al.*, *In Press*

## 7.5 CONCLUSION

Three of the five intravascular anticoagulation mechanisms (endothelial lining; AT III and heparin) and the normal coagulation pathway (decrease in F VII, X and VIII as described in chapter 5 of this thesis) were adversely affected by treatment with aspartame, either directly or indirectly. The effects of aspartame on the coagulation system, indirectly leading to decreased concentrations of thrombin (confirmed by results obtained on the platelet aggregation, chapter 6 of the thesis) affect coagulation which could lead to bleeding disorders. The intravascular anticoagulation system was also affected by treatment with aspartame, both directly (endothelial lining) and indirectly (no secretion of heparin or AT III). Thus it would seem as though an immune response was triggered by the administering of aspartame (increase in eosinophils, no



increase in basophils). The rabbits treated with aspartame also appeared to have suppressed immunity, as indicated by an overall decrease in the amount of leukocytes counted (Table 7.3). The effect of the decrease in the coagulation factors (bleeding disorders) causes decreased coagulation. A further decrease in coagulation was probably prevented by the increase in eosinophils which hindered the secretion of heparin from mast cells. Thus, AT III was also not increased to prevent a further decrease in coagulation.

The decreased amount of circulating thrombin, as indicated indirectly affects the concentration of serotonin (degranulation of platelets, Chapter 6). As seen from the summary and explanation, phenylalanine (one of metabolic constituents of aspartame) also decreases the amount of serotonin by preventing the conversion of tryptophan to serotonin. It was also shown that serotonin plays an integral part in the complexity of the tight junctions between two adjacent endothelial cells by attenuating the activity of cAMP. Thus it is hypothesized that aspartame compromises the BBB as the endothelial cells were apoptotic (TEM) and the amount of circulating serotonin decreased (decreased platelet aggregation as seen with SEM) affecting the complexity of the tight junctions by lowering the activity of cAMP.

This chapter therefore concludes that a defence mechanism exists within individuals and that the effect of aspartame on the normal coagulation, leukocyte numbers and intravascular anticoagulation system are in balance. This would however, not be the case with individuals genetically predisposed towards bleeding disorders. It is hypothesized that aspartame will affect normal coagulation and circulating concentrations of coagulation factors to a much higher degree in people with bleeding tendencies, and the effects caused by aspartame will not be balanced by the normal intravascular anticoagulation mechanisms, even if no AT III or heparin is secreted. Also, that using aspartame at abuse doses (150mg/kg aspartame and above) could lead to suppressed immunity (lowered counts of leukocytes), bleeding disorders (decreased coagulation) and a possible compromised BBB (lowered activity of cAMP due to decrease in serotonin).